Inorg. Chem. **2006**, *45*, 9053–9063

Reaction of $[Fe_2(CO)_8(\mu\text{-}CF_2)]$ with $AsMe_3$ and Other Lewis Bases: Syntheses, Crystal Structures of $[Fe(CO)_6(AsMe_3)_2(\mu\text{-}CF_2)]$ and $[Fe(CO)_5(AsMe_3)_3(\mu\text{-}CF_2)]$, and Theoretical Considerations

Meritxell DelaVarga,[†] Wolfgang Petz,*[,‡] Bernhard Neumüller,[‡] and Ramon Costa*[,†]

Departament de Química Inorgànica, Universitat de Barcelona, Martí i Franquès 1-11, E-08028 Barcelona, Spain, and Fachbereich Chemie der Philipps-Universität Marburg, Hans-Meerwein-Strasse, D-35032 Marburg, Germany

Received March 9, 2006

The difluorcarbene complex $[Fe_2(CO)_8(\mu\text{-}CF_2)]$ (**2**) reacts with $AsMe_3$ under CO substitution to give the μ-CF_2 containing complexes $[Fe_2(CO)_6(AsMe_3)_2(\mu\text{-}CF_2)]$ (**4**) and $[Fe_2(CO)_5(AsMe_3)_3(\mu\text{-}CF_2)]$ (**5**) which have an $[Fe_2(CO)_9]$-like structure as shown by X-ray analyses. In the solid state, **4** forms two isomers, **4a** and **4b**, in a 3 to 1 ratio, which differ in the position of the μ-CF_2 ligand; **4a** has a local C_2 axis and **4b** has C_1 symmetry. The Fe–Fe distances in **4** and **5** are 2.47 Å and are the shortest ones found in $[Fe_2(CO)_9]$-like compounds. Efforts were also undertaken to replace one or more CO groups in **2** by other ligands, such as N (bpy, phen, pzy, etc.) or P donors (dppe, dppm). With dppm, only the CF_2 free complex, $[Fe_2(CO)_4(\mu\text{-}Ph_2PCH_2PPh_2)_2(\mu\text{-}CO)]$ (**6**), could be detected and characterized by X-ray analysis. Most of the reactions resulted in the formation of red-brown materials which were insoluble in the usual solvents and which could not be characterized. The use of CH_2Cl_2 during the attempts to crystallize a product from the reaction of **2** and phen gave $[Fe(phen)_3]Cl_2$ (**7**) in low yields. For **4** and **5**, the electronic structures were analyzed using the atoms in molecules (AIM) theory. No electron density was found between the two iron atoms, and the short contacts can be interpreted in terms of a π-interaction.

Introduction

$[Fe_2(CO)_9]$ is an unique and fascinating molecule in organometallic chemistry containing six terminal and three bridging carbonyl groups.[1] The question of a direct Fe−Fe interaction is a controversial issue with answers ranging from yes[2] to no,[3] and the membership of publishers to one of the groups is expressed in drawing or omitting a line between the two metal atoms. However, it is commonly accepted that a subtle balance between the metal to carbonyl bridge bonding, metal−metal bonding, and intermetallic repulsion is operative.[3] Because of the high symmetric structure, the golden color, and the insolubility in organic solvents, as well as the ability to act as the source for the highly reactive 16-electron fragment $(CO)_4Fe$, the compound has gained the interest of generations of chemists.

The idea of substituting one or more carbonyl groups in $[Fe_2(CO)_9]$ by other isolobal 2-electron σ-donor/π-acceptor systems, D, and of exploring the structural changes occuring upon variation of D is very old and has inspired many chemists. However, no simple series of $[Fe_2(CO)_{9-x}(D)_x]$ compounds could be prepared. If one or more terminal or bridging CO groups are replaced, the series of compounds **A**−**C** (**A** has terminal D units, **B** has bridging D units, and **C** has terminal and bridging D units) should be obtained, and the structural options in the solid state are either an $[Fe_2(CO)_9]$-like structure (**I**) or an $[Os_2(CO)_9]$-like structure (**II**) as depicted in Chart 1.[4] For the type **A** compounds, a series of chelating phosphine ligands, such as $R_2PCH_2PR_2$,[5,6] R_2POPR_2,[7] R_2PNHPR_2,[8] $F_2PNMePF_2$,[9] and 1,2-diazine,[10] bridge the two Fe atoms to give $[Fe_2(CO)_7(D-D)]$ or $[Fe_2(CO)_5$-

* To whom correspondence should be addressed: E-mail: petz@staff.uni-marburg.de (W.P.); rcosta@ub.edu (R.C.).
† Universitat de Barcelona.
‡ Fachbereich Chemie der Philipps-Universität Marburg.

(1) Cotton, F. A.; Troup, J. M. *J. Chem. Soc., Dalton Trans.* **1974**, 800.
(2) (a) Mealli, C.; Proserpio D. M. *J. Organomet. Chem.* **1990**, *386*, 203. (b) Reinhold, J.; Hunstock, E.; Mealli, C. *New. J. Chem.* **1994**, *18*, 465.
(3) (a) Summerville, R. H.; Hoffmann, R. *J. Am. Chem. Soc.* **1979**, *101*, 3821. (b) Bauschlicher, C. W. *J. Chem. Phys.* **1986**, *84*, 872. (c) Rosa, A.; Baerends, E. *New. J. Chem.* **1991**, *15*, 815.
(4) Moss, J. R.; Graham, W. A. G. *Chem. Commun.* **1970**, 835.
(5) Cotton, F. A.; Troup, J. M. *J. Am. Chem. Soc.* **1974**, *96*, 4422.
(6) Wong, W. K.; Chiu, K. W.; Wilkinson, G.; Motevalli, M.; Hursthouse, M. B. *Polyhedron* **1985**, *4*, 1231.

10.1021/ic0604011 CCC: $33.50
Published on Web 09/27/2006

Chart 1. Derivatives of $Fe_2(CO)_9$[a]

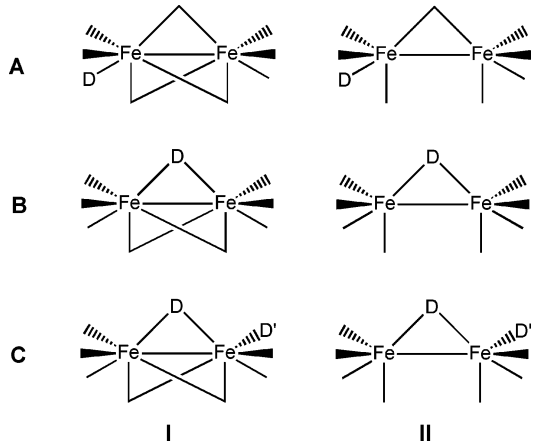

[a] **A** : One or more D ligands in terminal positions. **B**: One or more D ligands in bridging positions. **C**: D ligands in bridging and terminal positions. **I**: $Fe_2(CO)_9$-like structure. **II**: $Os_2(CO)_9$-like structure.

$(D-D)_2$] compounds which exhibit structure type **II**. However, aromatic chelating amine ligands, such as bpy,[11,12] phen,[12] or a chelating diarsine,[13] are attached at one iron atom generating two electronically different atoms, and the charge is balanced by the formation of asymmetrically bridging or semibridging CO groups; structures closely related to type **A-I** are observed.

To our knowledge, no type **A** compounds $[Fe_2(CO)_{6-x}(D)_x(\mu\text{-}CO)_3]$ with a single two-electron donor (NR_3, PR_3, or related bases) are known, but several type **B** compounds $[Fe_2(CO)_6(\mu\text{-}CO)_{3-x}(\mu\text{-}D)_x]$ are known. Therefore, we concentrate on compounds containing the two-electron donor molecules CR_2, [14] CF_2,[15] $C(CF_3)_2$, $C{=}CF_2$,[16] SiR_2, SnR_2,[17] $GeMe_2$,[18] SO_2,[19] and derivatives of low-valent group 13 compounds, such as InR,[20,21] GaR,[22] and TlR.[23] If only one μ-D ligand is present ($x = 1$), structure type **I** is found with

Chart 2. Bonding Situation in **2** with Two Semibridging CO Groups.

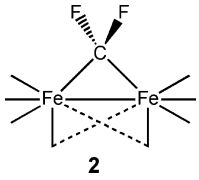

2

$D = CH_2$, while larger ligands prefer the structure type **II**. The Fe−Fe distances in the type **I** complexes range from 2.47 to 3.00 Å depending on the nature of the bridging ligand. With two[15] or three[20,23] μ-D ligands, a type **I** structure is formed. However, to our knowledge, no $[Fe_2(CO)_{6-y}(D')_y(CO)_{3-x}(\mu\text{-}D)_x]$ complex of type **C-I** has been known up to now, with the exception of CO-free $[Fe_2(CNEt)_6(\mu\text{-}CNEt)_3]$.[24] In all cases, the Fe−Fe distances in type **II** species are appreciably longer than those in type **I** compounds.

Recently, we have described the syntheses and crystal structures of compounds with the bridging difluorocarbene ligand.[15] While the structure of $[Fe_2(CO)_7(\mu\text{-}CF_2)_2]$ (**1**) is closely related to that of $[Fe_2(CO)_9]$ (**B-I**), with a very short Fe−Fe distance of 2.47 Å, the complex $[Fe_2(CO)_8(\mu\text{-}CF_2)]$ (**2**) exhibits no bridging CO groups according to the IR spectrum in either the solid state or solution down to −123 C°.[25] The crystal structure of **2**, which shows the presence of two semibridging CO groups**,** was interpreted in terms of being located between **B-I** and **B-II**, as shown in Chart 2.

The CF_2 ligand is a better acceptor than CO;[15,26] this is indicated by a shift of the ν(CO) vibrations to higher wavenumbers relative to those in $[Fe_2(CO)_9]$. It is therefore expected that the introduction of a better σ-donor in a terminal position should have a stabilizing effect.

As reported earlier, the addition of PPh_3 to **2** generates the disubstituted complex $[Fe_2(PPh_3)_2(CO)_6(\mu\text{-}CF_2)]$ (**3**) with a type **C-II** structure, and the phosphine ligands at both iron atoms are arranged in an asymmetrical form.[15]

The easy access to **3** prompted us to study the possibility of replacing CO by other donor molecules in more detail using various types of monodentate or chelating ligands. In particular, we studied the reaction of **2** with $AsMe_3$, As^iPr_3, dppe, dppm, and the α-diimines, bpy (2,2′-bipyridine), phen (1,10-phenantroline); we also studied it with pyrazine (pyz) and 4,4′-bpy. The results of our investigations are reported here. The electronic structures of the $AsMe_3$ derivatives obtained were analyzed using the atoms in molecules (AIM) theory.

Results and Discussion

In contrast to $[Fe_2(CO)_9]$, complex **2** is very soluble in the common solvents. Thus, in most cases, we used THF, toluene, or both as the solvent at room temperature, or the

(7) De Leeuw, G.; Field, J. S.; Haines, R. J.; McCulloch, B.; Meintjies, E.; Monberg, C.; Oliver, G. M.; Ramdial, P.; Sampson, C. N.; Sigwarth, B.; Stehen, N. D. *J. Organomet. Chem.* **1984**, *275*, 99.
(8) Ellermann, J.; Gabold, P.; Knoch, F. A.; Moll, M.; Pohl, D.; Sutter, J.; Bauer, W. *J. Organomet. Chem.* **1996**, *525*, 89.
(9) (a) Newton, M. G.; King, R. B.; Chang, M.; Gimeno, J. *J. Am. Chem. Soc.* **1977**, *99*, 2802. (b) Brown, G. M.; Finholt, J. E.; King, R. B.; Bibber, J. W.; Kim, J. H. *Inorg. Chem.* **1982**, *21*, 3790.
(10) Cotton, F. A.; Hanson, B. E.; Jamerson, J. D.; Stults, B. R. *J. Am. Chem. Soc.* **1977**, *99*, 3293.
(11) Cotton, F. A.; Troup, J. M. *J. Am. Chem. Soc.* **1974**, *96*, 1233.
(12) DelaVarga, M.; Costa, R.; Reina, R.; Nunez, A.; Maestro, M. A.; Mahia, J. *J. Organomet. Chem.* **2003**, *677*, 101.
(13) Bailey, W. I.; Bino, A.; Cotton, F. A.; Kolthammer, W. S.; Lahuerta, P.; Puebla, P.; Uson, R. *Inorg. Chem.* **1982**, *21*, 289.
(14) (a) Meyer, B. B.; Riley, P. E.; Davis, R. E. *Inorg. Chem.* **1981**, *20*, 3024. (b) Mills, O. S.; Redhouse, A. D. *J. Chem. Soc. A* **1968**, 1282.
(15) Petz, W.; Weller, F.; Barthel, A.; Mealli, C.; Reinhold, J. *Z. Anorg. Allg. Chem.* **2001**, *627*, 1859.
(16) (a) Wiederhold, M.; Behrens, U. *J. Organomet. Chem.* **1994**, *476*, 101. (b) Schulze, W.; Seppelt, K. *Inorg. Chem.* **1988**, *27*, 3872.
(17) Cardin, C. J.; Cardin, D. J.; Convery, M. A.; Devereux, M. M.; Tamley, B.; Silver, J. *J. Chem. Soc., Dalton Trans.* **1996**, 1145.
(18) Simons, R. S.; Tessier, C. A. *Acta Crystallogr., Sect. C* **1995**, *51*, 1997 and references therein.
(19) Meunier-Piret, J.; Piret, P.; Van Meerssche, M. *Bull. Soc. Chim. Belges* **1967**, *76*, 374.
(20) (a) Uhl, W.; Keimling, S. U.; Pohlmann, M.; Pohl, S.; Saak, W.; Hiller, W.; Neumeyer, M. *Inorg. Chem.* **1997**, *36*, 5478. (b) Uhl, W.; Pohlmann, M. *Organometallics* **1997**, *16*, 2478.
(21) Petz, W.; Esser, M.; Neumüller, B. *Z. Anorg. Allg. Chem.* **2006**, in press.
(22) (a) Jutzi, P.; Neumann, B.; Reumann, G.; Stammler, H.-G. *Organometallics* **1998**, *17*, 1305. (b) Uhl, W.; El-Hamdan, A.; Petz, W.; Geiseler, G.; Harms, K. *Z. Naturforsch.* **2004**, *59b*, 789. (c) Linti, G.; Köstler, W. *Chem. Eur. J.* **1998**, 942. (d) Linti, G.; Li, G.; Pritzkow, H. *J. Organomet. Chem.* **2001**, *626*, 82.
(23) Whitmire, K. H.; Guzman Jimenez, I. Y.; Saillard, J.-Y.; Kahlal, S. *J. Organomet. Chem.* **2000**, *614*, 243.
(24) Bassett, J.-M.; Green, M.; Howard, J. A. K.; Stone, F. G. A. *J. Chem. Soc., Chem. Commun.* **1978**, 1000.
(25) Grevels, F. W. Personal communication.
(26) Brothers, P. I.; Roper, W. R. *Chem. Rev.* **1988**, *88*, 1293.

Table 1. IR Frequencies (in Nujol mull, cm^{-1}) of **2**, **4**, and **5** in the ν(CO) and ν(CF) Region

compound	ν(CO)	$\nu(CF_2)$
$[Fe_2(\mu\text{-}CF_2)(CO)_8]$ (**2**)	2066 s, 2039 s, 2016 s, 1950 s	1034 m, 997 s
$[Fe_2(\mu\text{-}CF_2)(CO)_6(AsMe_3)_2]$ (**4**)	2038 m, 2004 s, 1971 s, 1940 vs, 1878 m, 1790 s	1018 m, 902 s
$[Fe_2(\mu\text{-}CF_2)(CO)_5(AsMe_3)_3]$ (**5**)	2036 w, 2000 m, 1982 s, 1944 vs, 1878 vw, 1818 w, 1786 m, 1766 m	1016 m, 900 m

Chart 3. Position of the $AsMe_3$ Ligands in **4a**, **4b**, and **5** with Terminal and Bridging CO Groups

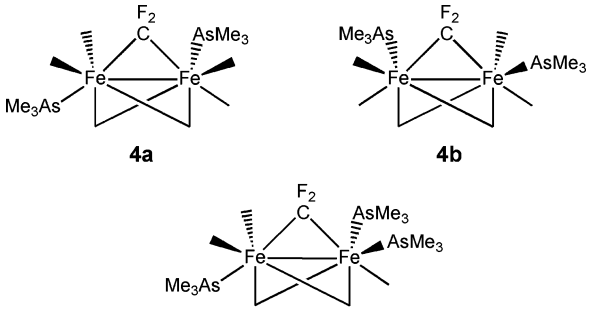

reaction was started at low temperature. With the majority of bases we introduced, red-brown precipitates formed, and the remaining red-brown solutions showed more than one signal in the ^{19}F NMR spectra (and in the ^{31}P NMR spectra in the case of P donors). From the intensities of the signals, it was clear that nearly all the reaction products were concentrated in the precipitates which were insoluble in the usual organic solvents; in some cases, no NMR signals could be obtained from these solutions. No reaction of **2** with acetonitrile and pyz was found. However, in the case of $AsMe_3$, we could isolate and characterize substituted compounds still containing the bridging CF_2 ligand. New complexes $[Fe_2(CO)_6(AsMe_3)_2(\mu\text{-}CF_2)]$ (**4**) and $[Fe_2(CO)_5(AsMe_3)_3(\mu\text{-}CF_2)]$ (**5**) were obtained in low yields and are the first examples of substituted $[Fe_2(CO)_9]$ derivatives in which structure type **C-I** is achieved (Chart 3). Complex **4** turned out to be a mixture of the isomers **4a** and **4b** in the solid state.

While the presence of the CF_2 groups in **1** and **2** causes a shift of the ν(CO) vibrations to higher frequencies with respect to $[Fe_2(CO)_9]$, according to the better π-acceptor properties of CF_2,[15] the introduction of the $AsMe_3$ ligands causes a shift in the reverse direction, and the frequencies are now located below those of $[Fe_2(CO)_9]$. The three ligands in **5** are more effective than the two ligands in **4**. Thus, the better σ-donor/π-acceptor relation of $AsMe_3$ overcompensates for the low σ-donor/π-acceptor relation of CF_2 with more electron density moving into π*-orbitals of the CO groups. In Table 1, the ν(CO) and $\nu(CF_2)$ frequencies of **4** and **5** are compared with those of **2**. The introduction of the $AsMe_3$ ligands causes also the $\nu(CF_2)$ bands in **4** and **5** to shift to lower frequencies, according to the enhanced electron density in the complexes and the decreasing CF double bond character. This is in accordance with the results of the crystal structure analysis showing longer C−F distances.

We also tried to prepare complexes with the more bulky $AsPr^i_3$ ligand. The reaction proceeded in ether with the formation of a red-brown precipitate; however, efforts to redissolve the precipitate in an appropriate solvent for further characterization were unsuccessful. The solid showed ν(CO) frequencies at 2042 m, 2010 w, 1986 w, 1966 m, 1931 vs, and 1862 s cm^{-1}, and the remaining solution showed a signal at 42 ppm in the ^{19}F NMR spectrum. No crystals for structural characterization could be obtained.

Similarly, chelating phosphine ligands such as $Ph_2PCH_2PPh_2$ (dppm) or $(Ph_2PCH_2)_2$ (dppe) react slowly with **2** in toluene to produce brown to red-brown precipitates. However, attempts to recrystallize the materials by dissolving them in various solvents have failed. Most of the material was insoluble and probably consisted of a mixture of products. In some cases, however, we could isolate few red crystals which were identified as $[Fe_2(CO)_4(\mu\text{-}Ph_2PCH_2PPh_2)_2(\mu\text{-}CO)]$ (**6**), but no crystalline compound containing a CF_2 group was identified, and the whereabouts of this group is still unclear. The lack of any ^{19}F NMR signal in some solutions of the reaction products indicate that the CF_2 ligand must be incorporated in the insoluble parts. It seems that the presence of the strongly bonded CF_2 bridge prevents, in most cases, the formation of a substituted $[Fe_2(CO)_9]$-like complex. The ^{19}F NMR of the solution of **2** with dppm showed a peak at about 42 ppm; in the ^{31}P NMR spectrum, a main signal at 60 ppm and others at 85, 62, and 20 ppm were found. Similarly, the remaining solutions (after removal of the precipitate) of the reaction of **2** with dppe gave one signal at 35 ppm in the ^{19}F NMR spectrum, and in the ^{31}P NMR spectrum, a singlet at 96 ppm, together with multiplets at 70, 52 and 28 ppm, was observed.

The use of CH_2Cl_2 as a solvent in the reaction of **2** with phen gave a crystalline compound which, however, was identified as the oxidation product $[Fe(phen)_3]Cl_2$ (**7**). It is known that CH_2Cl_2 can act as an oxidation agent toward low-valent carbonyl compounds.[27] In one of the recrystallization procedures, we have also obtained $[Fe(CO)_3(phen)]$.[12]

No reaction of **2** with acetonitrile and pyz was found. When TMNO was added as initiator for CO activation,[12] the known trinuclear complex $[Fe_3(CO)_9(\mu_3\text{-}CF)_2]$ was obtained.[28] This product was also formed if **2** was allowed to react with TMNO alone, but when other ligands were present (dppe, bpy, or phen), $[Fe_3(CO)_9(\mu_3\text{-}CF)_2]$ was not detected.

During our studies of the chemistry of **2**, it turned out that CO groups cannot simply be replaced by other donor ligands. Thus, as yet, the earlier reported complex **3** and the compounds **4** and **5** in this contribution are the only known substitution products of **2** established by X-ray analyses.

Crystal Structures. General Remarks. To obtain more insight into the properties of the compounds, the structures

(27) Petz, W.; Weller, F. *Z. Naturforsch.* **1991**, *46b*, 297.
(28) Lentz, D.; Brüdggam, I.; Hartl, H. *Angew. Chem., Int. Ed. Engl.* **1985,** *24,* 119.

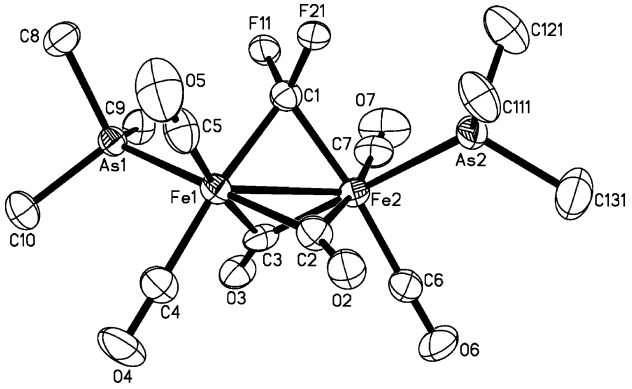

Figure 1. Projection view of **4a** with the labeling scheme (30% ellipsoids). The hydrogen atoms have been omitted for clarity.

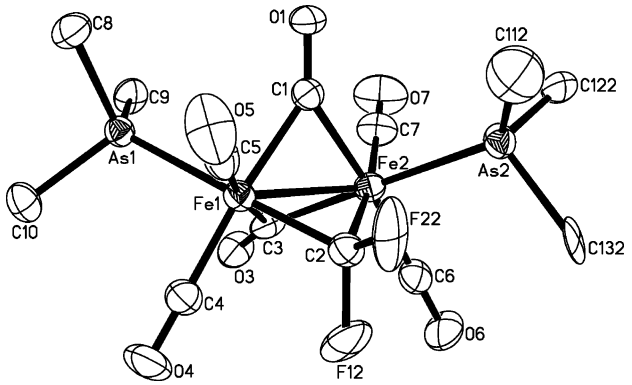

Figure 2. Projection view of **4b** with the labeling scheme (30% ellipsoids). The hydrogen atoms have been omitted for clarity.

of **4**, **5**, and **6** have been determined by single-crystal X-ray diffraction measurements. The synthesis of **6** was described earlier,[7] and the crystal structures of the solvates **6**·OC(Me)$_2$ [29] and **6**·2MeC$_6$H$_5$ [30] were obtained. In our case, **6** crystallizes as a toluene solvate but with only one solvent molecule. We also present the crystal structure of [Fe(phen)$_3$]Cl$_2$ (**7**) which we obtained during the attempts to recrystallize the red material from the reaction of **2** with phen in CH_2Cl_2. ORTEP views of molecules **4a**, **4b**, and **5** are depicted in Figures 1−3, respectively; Figure 4 shows the crystal structure of the cation of **7**. Details of the structure determinations are collected in Table 2, and the bond distances and angles are summarized in Table 3.

Crystal Structure of [Fe$_2$(CO)$_6$(μ-CF$_2$)(AsMe$_3$)$_2$] (4a and 4b). In contrast to **3**, where a **C-II** structure type is found, the presence of two AsMe$_3$ ligands allows the isolation of the first compounds of type **C-I**. In the solid state, **4** was found to be a superposition of the chiral isomers **4a** and **4b** with 75 and 25% distributions, and the molecular structures are depicted in Figures 1 and 2, respectively. The disorder of the methyl groups at As(2) probably coincides with the disorder of the CF_2 position. The major isomer **4a** has approximately a local molecular C_2 axis through C(1) of the CF_2 group and the middle of the Fe−Fe bond; **4b** has C_1 symmetry. The Fe−Fe distance in **4** amounts to 2.47 Å and

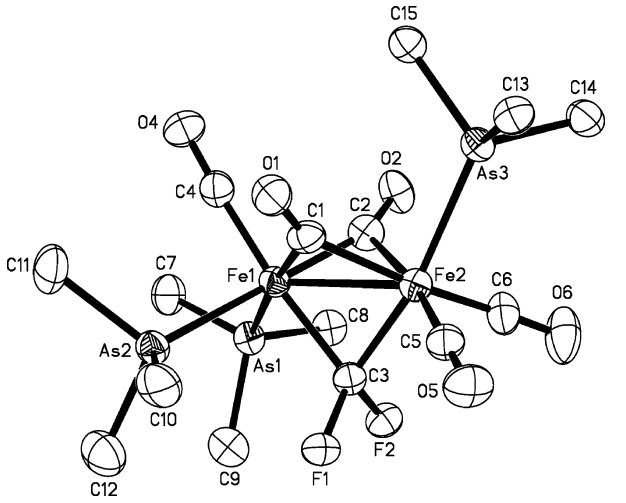

Figure 3. Projection view of **5** with the labeling scheme (30% ellipsoids). The hydrogen atoms have been omitted for clarity.

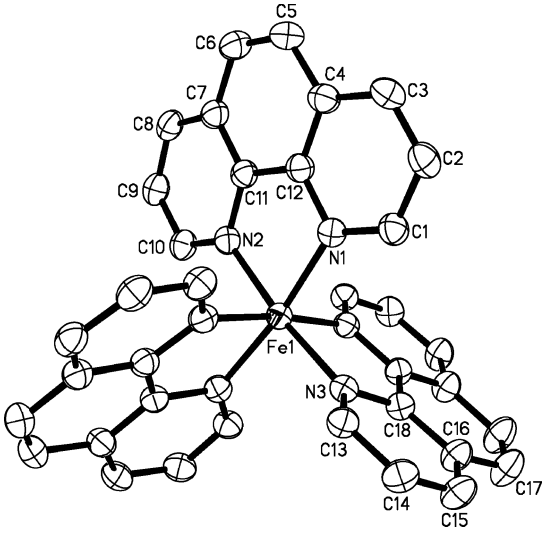

Figure 4. Projection view of the cation of **7** with the labeling scheme (40% ellipsoids). The hydrogen atoms have been omitted for clarity.

is the shortest one found in the related type **I** complexes; a similar short distance is also found in **1**.[15] It is the same in **5** and apparently not influenced by the number and nature of the terminal non-CO ligands. When the predominate isomer, **4a**, is considered, the bridging CO(3) ligand, which is not involved in the disorder, and the other bridging CO(2) group form asymmetric bonds to the iron atoms. Both CO groups have one AsMe$_3$ ligand and one terminal CO in the trans position. The short Fe−CO distances (1.90 Å) are directed toward the *trans*-AsMe$_3$ groups, while the longer ones (2.04 Å) are opposite to the CO groups. The Fe−As distances are nearly equal at 2.371 and 2.378 Å, but they are about 0.07 Å longer than in the mononuclear arsine complex [(CO)$_4$FeAsMe$_3$].[31] The F−C−F angles of **4a** and **4b** are equal (101°) and identical with that of the starting complex **2**. Along the Fe(1)−Fe(2) connection, the ligands form approximately three planes. The terminal and bridging ligands are staggered as in [Fe$_2$(CO)$_9$], and the ligand

(29) Moodley, K. G.; Engel, D. W.; Field, J. S.; Haines, R. J. *Polyhedron* **1993**, *12*, 533.
(30) Hitchcock, P. B.; Madden, T. J.; Nixon, J. F. *J. Organomet. Chem.* **1993**, *463*, 155.
(31) Legendre, J.-J.; Girard, C.; Huber, M. *Bull. Soc. Chim. Fr.* **1971**, 1998.

Table 2. Experimental Data for the X-ray Diffraction Studies of Complexes **4**, **5**, **6**·MeC_6H_5, and **7**

	4	**5**	**6**·MeC_6H_5	**7**
formula	$C_{13}H_{18}As_2F_2Fe_2O_6$	$C_{15}H_{27}As_3F_2Fe_2O_5$	$C_{62}H_{52}Fe_2O_5P_4$	$C_{38}H_{28}Cl_6N_6Fe$
mol wt	569.81	661.83	1112.68	837.25
cryst syst	orthorhombic	orthorhombic	triclinic	monoclinic
space group	*Pbca* (No. 61)	$Pna2_1$ (No. 33)	$P\bar{1}$ (No. 2)	$I2/a$ (No. 15)
a (Å)	14.411(1)	14.213(1)	12.173(2)	19.185(2)
b (Å)	11.368(1)	16.597(2)	12.587(2)	10.781(1)
c (Å)	24.717(1)	10.070(1)	19.775(3)	18.466(1)
α (deg)	90	90	70.96(1)	90
β (deg)	90	90	71.88(1)	103.69(1)
γ (deg)	90	90	70.66(1)	90
vol ($\times 10^6$ pm^3)	4049.2(6)	2375.4(4)	2631.7(1)	3710.9(6)
Z	8	4	2	4
d_{calcd} (g/cm^3)	1.869	1.851	1.404	1.499
temp (K)	193	193	193	193
μ(Mo Kα) (cm^{-1})	47.2	54.0	7.2	
R_1 ($F_0 > 4\sigma F_0$)[a]	0.0251	0.0479	0.0692	0.0419
R_2 (all data)	0.0320	0.1176	0.1496	0.1222

[a] refinement: SHELXL-97,[32] structure solution, direct methods, SHELXS-97.[33]

arrangements in **4a** and **4b** are sketched in Charts 4 and 5, respectively. Each Fe atom is in an approximately octahedral environment.

Crystal Structure of $[Fe_2(CO)_5(\mu\text{-}CF_2)(AsMe_3)_3]$ (5). Complex **5** represents a further example of the **C-I** type and contains three terminal $AsMe_3$ groups making the two Fe atoms electronically different. The Fe−Fe distance is (2.471 Å) as short as in **4**. The Fe atoms and the CF_2 group form a slightly asymmetric triangle with Fe−C bond lengths of 1.978 (Fe(1)) and 1.930 Å (Fe(2)), respectively. The dihedral angle between the planes $Fe_2C(1)$ and $Fe_2C(3)$ is 125°; the other dihedral angles are nearly equal with values of 118 and 117°, respectively. Two Fe−As distances are equal (2.364 Å), but one of the two Fe−As distances at the same side (As(2)) is about 0.05 Å longer which may be the result of packing effects; related Fe−As distances of 2.36 and 2.34 Å were also measured in the $[(diars)Fe_2(CO)_7]$ complex in which the chelating ligand, *o*-phenylenebis(dimethylarsine), is coordinated at one Fe atom.[8] The mean C−F distance of 1.39 Å is appreciably longer than the related distance in **2** (1.36 Å); the same trend that was observed for the CO ligands is observed here. All Fe−As distances in **5** are about 0.06−0.11 Å longer than in the mononuclear arsine complex $[(CO)_4FeAsMe_3]$ (2.30(3) Å),[31] indicating less back-bonding into the As atoms in the dinuclear complex; a similar trend is observed with the Fe−P distances in comparing the $[(CO)_4FePPh_3]$[32] compounds with **3**.[15] Along the Fe(1)−Fe-(2) connection, three planes perpendicular to this can be defined with terminal, bridging, and terminal ligands, as depicted in Chart 6 (superposition of the planes 1, 2, and 3); two $AsMe_3$ groups are arranged cis to the CF_2 ligand (plane 1), and the unique $AsMe_3$ group (plane 3) is trans to the CF_2 group and trans to the middle of the other $AsMe_3$ groups in plane 1. The As(1)−Fe(1)−Fe(2) and As(2)−Fe-(1)−Fe(2) angles are different with values of 125.8 and 115.6°, respectively. The $Fe_2C(CF_2)$ containing triangle, one terminal CO group at Fe(1), and the As(3) atom are located within the non-crystallographic symmetry plane. At Fe(1), the two $AsMe_3$ groups are located trans to the bridging carbonyl groups. The As(1)−Fe(1)−As(2) angle is about 11° larger than that in $[(diars)Fe_2(CO)_7]$,[8] where the five-membered ring forces the As atoms closer together. Both the bridging carbonyl groups, CO(1) and CO(2), show tendencies to form pairwise asymmetric bridges, especially CO(2), which is located opposite of the long As(2), and tends nearly toward a semibridging CO group at Fe(1) forming a long C(2)−Fe(2) distance of 2.161 Å. This is supported by the different Fe(1)−C(2)−O(2) and Fe(2)−C(2)−O(2) angles of 152 and 131°, respectively. The geometrical classifications made earlier[11,33,34] coincide with consideration of the CO(1) ligand as an asymmetric bridging carbonyl group and CO-(2) as a semibridging one.

The F(1)−C(3)−F(2) angle is more acute than in the starting complex **2**. If the Fe−Fe-interaction is ignored, the coordination at each Fe atom is nearly octahedral with two octahedrons sharing one face.

Crystal Structure of $[Fe_2(\mu\text{-dppm})_2(CO)_5]\cdot MeC_6H_5$ (6·MeC_6H_5). For the type $[Fe_2(CO)_5(D-D)_2]$ compounds, crystal structures have been published from compounds with D−D = $R_2P-Y-PR_2$, where R = Me, Y = CH_2;[6] R = OEt Y = O;[35] R = F, Y = NEt;[9] and R = Ph, Y = NH,[8] CH_2.[29,30] From compounds with R = Ph, Y = CH_2 (as in **6**), the solvates **6**·$2Me_2CO$[29] and **6**·$2MeC_6H_5$ [30] were described, whereas in our case, the monotoluene solvate **6**·MeC_6H_5 has formed. The different numbers and types of solvent molecules incorporated have some influence on the parameters of the molecule. Whereas for **6**·$2MeC_6H_5$, a crystallographic mirror plane and an Fe−Fe separation of 2.711 Å were found,[30] no mirror plane and a long Fe−Fe distance of 2.740 Å were measured in **6**·MeC_6H_5; the other distances and angles are nearly identical. The **6**·$2Me_2CO$ derivative has the same Fe−Fe separation[29] as our results, but all distances are about 0.03 to 0.06 Å longer, and most of the bond angles are far from those in **6**·MeC_6H_5. Within the series of $[Fe_2(CO)_5(D-D)_2]$ compounds for **6**·MeC_6H_5 the largest Fe−Fe distance is recorded. The structure is also closely related

(32) Riley, P. E.; Davis, R. E. *Inorg. Chem.* **1980**, *18*, 159.
(33) Colton, R.; McCormick, M. J. *Coord. Chem. Rev.* **1980**, *31*, 1.
(34) Cotton, F. A. *Prog. Inorg. Chem.* **1976**, *21*, 1.
(35) Cotton, F. A.; Haines, R. J.; Hanson, B. E.; Sekutowski, J. C. *Inorg. Chem.* **1978**, *17*, 2010.

Table 3. Selected Bond Distances (Å) and Angles (deg) in **4**, **5**, **6**·MeC_6H_5, and **7**

4a and **4b**

As(1)−Fe(1)	2.3782(6)	As(1)−C(8)	1.930(3)	Fe(1)−C(5)	1.775(4)	Fe(2)−C(1)	2.002(3)
As(1)−C(9)	1.932(3)	As(1)−C(10)	1.923(3)	Fe(2)−C(2)	2.036(3)	Fe(2)−C(3)	1.903(4)
As(2)−Fe(2)	2.3713(5)	As(2)−C(111)	1.950(6)	Fe(2)−C(6)	1.807(4)	Fe(2)−C(7)	1.769(4)
As(2)−C(121)	1.904(5)	As(2)−C(131)	1.908(6)	F(11)−C(1)	1.375(4)	F(21)−C(1)	1.382(4)
As(2)−C(112)	1.83(2)	As(2)−C(122)	1.86(2)	O(2)−C(2)	1.187(5)	O(3)−C(3)	1.175(4)
As(2)−C(132)	1.96(2)	Fe(1)−Fe(2)	2.4705(6)	O(4)−C(4)	1.141(4)	O(5)−C(5)	1.143(4)
Fe(1)−C(1)	1.978(3)	Fe(1)−C(2)	1.900(4)	O(6)−C(6)	1.140(3)	O(7)−C(7)	1.153(4)
Fe(1)−C(3)	2.044(3)	Fe(1)−C(4)	1.798(4)	F(12)−C(2)	1.40(1)	F(22)−C(2)	1.30(1)
O(1)−C(1)	1.18(1)						

Fe(1)−As(1)−C(8)	115.86(9)	Fe(1)−As(1)−C(9)	119.4(1)	As(2)−Fe(2)−C(1)	90.74(9)	As(2)−Fe(2)−C(2)	87.30(9)
Fe(1)−As(1)−C(10)	114.4(1)	C(8)−As(1)−C(9)	101.6(1)	As(2)−Fe(2)−C(3)	173.5(1)	As(2)−Fe(2)−C(6)	91.8(1)
C(8)−As(1)−C(10)	102.4(1)	C(9)−As(1)−C(10)	100.4(1)	As(2)−Fe(2)−C(7)	95.1(1)	Fe(1)−Fe(2)−C(1)	51.19(9)
Fe(2)−As(2)−C(111)	122.1(2)	Fe(2)−As(2)−C(121)	115.7(2)	Fe(1)−Fe(2)−C(2)	48.7(1)	Fe(1)−Fe(2)−C(3)	53.8(1)
Fe(2)−As(2)−C(131)	116.1(2)	Fe(2)−As(2)−C(112)	121.8(7)	Fe(1)−Fe(2)−C(6)	120.4(1)	Fe(1)−Fe(2)−C(7)	123.9(1)
Fe(2)−As(2)−C(122)	114.1(7)	Fe(2)−As(2)−C(132)	109.4(5)	C(1)−Fe(2)−C(2)	82.0(1)	C(1)−Fe(2)−C(3)	86.5(1)
C(111)−As(2)−C(121)	99.9(2)	C(111)−As(2)−C(131)	100.0(3)	C(1)−Fe(2)−C(6)	171.0(1)	C(1)−Fe(2)−C(7)	90.1(2)
C(121)−As(2)−C(131)	99.4(3)	C(112)−As(2)−C(122)	103.0(1)	C(2)−Fe(2)−C(3)	86.4(1)	C(2)−Fe(2)−C(6)	89.5(1)
C(112)−As(2)−C(132)	105.0(9)	C(122)−As(2)−C(132)	101.1(7)	C(2)−Fe(2)−C(7)	171.8(2)	C(3)−Fe(2)−C(6)	90.1(1)
As(1)−Fe(1)−Fe(2)	118.8(4)	As(1)−Fe(1)−C(1)	90.7(1)	C(3)−Fe(2)−C(7)	90.8(2)	C(6)−Fe(2)−C(7)	98.3(2)
As(1)−Fe(1)−C(2)	171.9(1)	As(1)−Fe(1)−C(3)	85.9(1)	Fe(1)−C(1)−Fe(2)	76.7(1)	Fe(1)−C(1)−F(11)	122.1(2)
As(1)−Fe(1)−C(4)	92.0(1)	As(1)−Fe(1)−C(5)	95.3(1)	Fe(1)−C(1)−F(21)	119.4(2)	Fe(1)−C(1)−O(1)	142.2(6)
Fe(2)−Fe(1)−C(1)	52.1(1)	Fe(2)−Fe(1)−C(2)	53.6(1)	Fe(2)−C(1)−F(11)	118.4(2)	Fe(2)−C(1)−F(21)	118.8(2)
Fe(2)−Fe(1)−C(3)	48.75(9)	Fe(2)−Fe(1)−C(4)	121.0(1)	Fe(2)−C(1)−O(1)	140.9(6)	F(11)−C(1)−F(21)	101.6(3)
Fe(2)−Fe(1)−C(5)	125.5(1)	C(1)−Fe(1)−C(2)	86.2(1)	Fe(1)−C(2)−Fe(2)	77.7(1)	Fe(1)−C(2)−O(2)	146.1(3)
C(1)−Fe(1)−C(3)	83.4(1)	C(1)−Fe(1)−C(4)	172.8(1)	Fe(1)−C(2)−F(12)	116.0(6)	Fe(1)−C(2)−F(22)	121.5(6)
C(1)−Fe(1)−C(5)	89.8(2)	C(2)−Fe(1)−C(3)	86.3(1)	Fe(2)−C(2)−O(2)	136.2(3)	Fe(2)−C(2)−F(12)	118.2(5)
C(2)−Fe(1)−C(4)	90.3(1)	C(2)−Fe(1)−C(5)	92.2(2)	Fe(2)−C(2)−F(22)	122.4(6)	F(12)−C(2)−F(22)	101.4(9)
C(3)−Fe(1)−C(4)	90.1(1)	C(3)−Fe(1)−C(5)	173.2(2)	Fe(1)−C(3)−Fe(2)	77.4(1)	Fe(1)−C(3)−O(3)	137.7(3)
C(4)−Fe(1)−C(5)	96.6(2)	As(2)−Fe(2)−Fe(1)	120.07(2)	Fe(2)−C(3)−O(3)	144.9(3)		

5

As(1)−Fe(1)	2.363(1)	As(1)−C(7)	1.92(1)	Fe(1)−C(4)	1.79(1)	Fe(2)−C(1)	1.938(9)
As(1)−C(8)	1.93(1)	As(1)−C(9)	1.92(1)	Fe(2)−C(2)	2.161(9)	Fe(2)−C(3)	1.930(8)
As(2)−Fe(1)	2.413(1)	As(2)−C(10)	1.94(1)	Fe(2)−C(5)	1.753(8)	Fe(2)−C(6)	1.73(1)
As(2)−C(11)	1.95(1)	As(2)−C(12)	1.93(1)	F(1)−C(3)	1.388(8)	F(2)−C(3)	1.391(9)
As(3)−Fe(2)	2.364(1)	As(3)−C(13)	1.936(8)	O(1)−C(1)	1.18(1)	O(2)−C(2)	1.19(1)
As(3)−C(14)	1.93(1)	As(3)−C(15)	1.936(9)	O(4)−C(4)	1.14(1)	O(5)−C(5)	1.17(1)
Fe(1)−Fe(2)	2.471(2)	Fe(1)−C(1)	2.005(9)	O(6)−C(6)	1.20(1)		
Fe(1)−C(2)	1.83(1)	Fe(1)−C(3)	1.978(8)				

Fe(1)−As(1)−C(7)	116.9(4)	Fe(1)−As(1)−C(8)	115.9(3)	C(2)−Fe(1)−C(3)	86.1(4)	C(2)−Fe(1)−C(4)	89.8(4)
Fe(1)−As(1)−C(9)	120.3(3)	C(7)−As(1)−C(8)	99.8(5)	C(3)−Fe(1)−C(4)	173.4(4)	As(3)−Fe(2)−Fe(1)	115.57(6)
C(7)−As(1)−C(9)	101.3(6)	C(8)−As(1)−C(9)	99.2(5)	As(3)−Fe(2)−C(1)	85.0(3)	As(3)−Fe(2)−C(2)	88.8(3)
Fe(1)−As(2)−C(10)	118.3(4)	Fe(1)−As(2)−C(11)	112.6(4)	As(3)−Fe(2)−C(3)	166.6(2)	As(3)−Fe(2)−C(5)	97.8(3)
Fe(1)−As(2)−C(12)	122.8(4)	C(10)−As(2)−C(11)	99.9(5)	As(3)−Fe(2)−C(6)	92.3(3)	Fe(1)−Fe(2)−C(1)	52.4(3)
C(10)−As(2)−C(12)	96.7(6)	C(11)−As(2)−C(12)	103.0(7)	Fe(1)−Fe(2)−C(2)	45.9(3)	Fe(1)−Fe(2)−C(3)	51.7(2)
Fe(2)−As(3)−C(13)	114.8(2)	Fe(2)−As(3)−C(14)	117.6(3)	Fe(1)−Fe(2)−C(5)	125.5(3)	Fe(1)−Fe(2)−C(6)	120.4(4)
Fe(2)−As(3)−C(15)	117.6(3)	C(13)−As(3)−C(14)	100.9(4)	C(1)−Fe(2)−C(2)	82.5(3)	C(1)−Fe(2)−C(3)	88.4(4)
C(13)−As(3)−C(15)	102.6(4)	C(14)−As(3)−C(15)	100.7(4)	C(1)−Fe(2)−C(5)	92.4(4)	C(1)−Fe(2)−C(6)	169.1(4)
As(1)−Fe(1)−As(2)	96.75(5)	As(1)−Fe(1)−Fe(2)	125.8(4)	C(2)−Fe(2)−C(3)	78.8(3)	C(2)−Fe(2)−C(5)	171.3(4)
As(1)−Fe(1)−C(1)	174.5(3)	As(1)−Fe(1)−C(2)	90.2(3)	C(2)−Fe(2)−C(6)	86.9(4)	C(3)−Fe(2)−C(5)	94.1(4)
As(1)−Fe(1)−C(3)	89.3(2)	As(1)−Fe(1)−C(4)	95.8(3)	C(3)−Fe(2)−C(6)	92.1(4)	C(5)−Fe(2)−C(6)	98.5(5)
As(2)−Fe(1)−Fe(2)	115.58(5)	As(2)−Fe(1)−C(1)	83.2(2)	Fe(1)−C(1)−Fe(2)	77.6(3)	Fe(1)−C(1)−O(1)	138.6(8)
As(2)−Fe(1)−C(2)	172.8(3)	As(2)−Fe(1)−C(3)	91.9(2)	Fe(2)−C(1)−O(1)	143.7(8)	Fe(1)−C(2)−Fe(2)	76.0(2)
As(2)−Fe(1)−C(4)	91.6(3)	Fe(2)−Fe(1)−C(1)	50.0(3)	Fe(1)−C(2)−O(2)	152.3(9)	Fe(2)−C(2)−O(2)	131.1(8)
Fe(2)−Fe(1)−C(2)	58.1(3)	Fe(2)−Fe(1)−C(3)	49.9(2)	Fe(1)−C(3)−Fe(2)	78.4(3)	Fe(1)−C(3)−F(1)	119.8(5)
Fe(2)−Fe(1)−C(4)	123.5(3)	C(1)−Fe(1)−C(2)	89.7(4)	Fe(1)−C(3)−F(2)	120.6(5)	Fe(2)−C(3)−F(1)	121.1(5)
C(1)−Fe(1)−C(3)	85.2(3)	C(1)−Fe(1)−C(4)	89.6(4)	Fe(2)−C(3)−F(2)	118.2(5)	F(1)−C(3)−F(2)	99.9(6)

6·MeC_6H_5

Fe(1)−Fe(2)	2.740(1)	Fe(1)−P(3)	2.218(2)	Fe(2)−P(4)	2.223(2)	Fe(2)−C(5)	1.783(7)
Fe(1)−P(1)	2.197(2)	Fe(1)−C(2)	1.723(7)	Fe(2)−C(4)	1.714(7)	P(4)−C(31)	1.833(7)
Fe(1)−C(1)	1.972(7)	Fe(2)−P(2)	2.227(2)	O(1)−C(1)	1.218(7)	P(3)−C(31)	1.831(7)
Fe(1)−C(3)	1.784(8)	Fe(2)−C(1)	1.957(6)				

P(1)−Fe(1)−P(3)	170.3(6)	P(1)−Fe(1)−C(1)	91.4(3)	P(4)−Fe(2)−C(5)	91.8(2)	C(1)−Fe(2)−C(4)	109.8(3)
P(1)−Fe(1)−C(2)	86.8(3)	P(1)−Fe(1)−C(3)	88.5(3)	C(1)−Fe(2)−C(5)	136.2(3)	C(4)−Fe(2)−C(5)	114.0(4)
P(3)−Fe(1)−C(1)	96.6(2)	P(3)−Fe(1)−C(2)	86.0(3)	Fe(1)−P(1)−C(6)	113.7(2)	Fe(1)−P(3)−C(31)	112.6(2)
P(3)−Fe(1)−C(3)	88.7(3)	C(1)−Fe(1)−C(2)	105.5(3)	Fe(2)−P(2)−C(6)	113.8(2)	Fe(2)−P(4)−C(31)	111.0(2)
C(1)−Fe(1)−C(3)	140.1(3)	C(2)−Fe(1)−C(3)	114.3(4)	Fe(1)−C(1)−Fe(2)	88.4(3)	Fe(1)−C(1)−O(1)	136.3(5)
P(2)−Fe(2)−P(4)	170.89(9)	P(2)−Fe(2)−C(1)	88.2(2)	Fe(2)−C(1)−O(1)	135.2(6)	P(1)−C(6)−P(2)	114.4(3)
P(2)−Fe(2)−C(4)	85.2(3)	P(2)−Fe(2)−C(5)	95.2(2)	P(3)−C(31)−P(4)	109.0(4)		
P(4)−Fe(2)−C(1)	90.8(2)	P(4)−Fe(2)−C(4)	86.6(3)				

Table 3. Continued

7

Fe(1)−N(1)	1.979(2)	Fe(1)−N(2)	1.987(2)	N(1)−C(12)	1.366(3)	N(3)−C(18)	1.366(3)
Fe(1)−N(3)	1.972(2)	N(2)−C(11)	1.365(3)	C(11)−C(12)	1.423(3)		
N(1)−Fe(1)−N(2)	82.45(7)	N(1)−Fe(1)−N(3)	92.24(7)	N(2)−Fe(1)−N(3a)	93.77(7)	N(3)−Fe(1)−N(3a)	82.60(7)
N(1)−Fe(1)−N(1a)	172.65(8)	N(1)−Fe(1)−N(2a)	92.35(7)	Fe(1)−N(1)−C(12)	112.6(1)	Fe(1)−N(1)−C(1)	130.4(2)
N(1)−Fe(1)−N(1a)	93.28(7)	N(2)−Fe(1)−N(3)	173.41(7)	Fe(1)−N(2)−C(10)	130.4(2)	Fe(1)−N(2)−C(11)	112.5(1)
N(2)−Fe(1)−N(1a)	92.35(7)	N(2)−Fe(1)−N(2a)	90.37(7)	Fe(1)−N(3)−C(18)	113.2(1)		

Chart 4. Arrangement of the Two $AsMe_3$ Ligands (**As**) in **4a** Looking down the Fe(1)−Fe(2) Connection (dotted line)

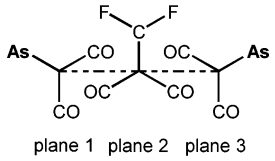

4a

Chart 5. Arrangement of the Two $AsMe_3$ Ligands (**As**) in **4b** Looking down the Fe(1)−Fe(2) Connection (dotted line)

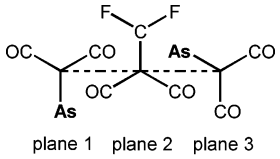

4b

Chart 6. Arrangement of the Three $AsMe_3$ Ligands (**As**) in **5** Looking down the Fe(1)−Fe(2) Connection (dotted line)

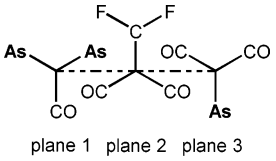

5

to that with R = Me (Y = CH_2),[6] but the Fe−Fe distance is 0.02 Å longer than in the methyl derivative which causes also elongation of the Fe(1)−C(1), Fe(2)−C(1), and C(1)−O(1) bonds lengths at the single bridging carbonyl group; similarly, this effect is observed concerning the Fe−P distances.

If only one chelating ligand is present, as in [$Fe_2(CO)_7(Ph_2PCH_2PPh_2)$],[5] the Fe−Fe distance is about 0.03 Å shorter, although no further bridging ligand forces the atoms together. Compared to this, the mean Fe−CO(terminal) distances in **6**·MeC_6H_5 are shorter, indicating enhanced π-back-bonding to the remaining CO groups in the presence of four weaker acceptor atoms. If the terminal carbonyl groups are considered to be inline with the Fe−Fe bond, they are more involved in back-bonding (Fe−C = 1.72 Å, C−O = 1.20 Å) than those perpendicular to the Fe−Fe bond (Fe−C = 1.78 Å, C−O = 1.18 Å).

Crystal Structure of [Fe(phen)₃]Cl₂ (7). The red compound crystallizes with two molecules of CH_2Cl_2. These and the Cl^- ions are connected via very weak hydrogen bonds with a Cl···C contact of 3.437(4) Å. No further contacts exist between the cation and the two anions. Complex **7** crystallizes in the centrosymmetric space group *I*2/*a*, and the dication lies on a C_2 axis and is shown in Figure 4. The planar rings Fe(1)−N(1)−C(12)−C(11)−N(2) and Fe(1)−N(3)−C(18)−C(18a)−N(3a) form an dihedral angle of 84°, and the N−Fe−N angles within the rings are 82.5°. The mean Fe(1)−N distance is 1.979(2) Å and is in a normal range.

Theoretical Studies. The Bader's atoms in molecules (AIM)[36−38] topological analysis of the molecular electronic density (obtained from ab initio calculations) has been used to study the bonding and structure properties of diiron nonacarbonyl[39] and some of its derivatives,[12] especially focusing on the Fe−Fe bond. The key point of Bader's theory is that a chemical bond must be characterized by the existence of a point on the internuclear bondpath line where the Hessian matrix of the total electronic density has one positive and two negative eigenvalues: this point is called a bond critical point (BCP), and we can imagine it as a bottleneck of electron density between the two bonded atoms. The values of the density, together with its Laplacian and the bond ellipticity (ρ, $\nabla^2\rho$ and ϵ respectively) at these points, give indications on how the bonding density is distributed along the internuclear line and aids in the bond characterization. Nevertheless, most works fail to find a BCP on the central part of the line joining the two iron nuclei; on the contrary, electronic density depletions corresponding to cage critical points (CCP)[39] or ring critical points (RCP)[12] are found at those regions. These findings suggest that the existence of a direct iron−iron bond through overlap over the internuclear line predicted by the 18-electron rule in this kind of complex[11] is doubtful and that dinuclear integrity is kept exclusively by the bridging carbonyl ligands. From that viewpoint, such dinuclear complexes consist of two iron coordination polyhedra sharing one face or one edge (see Chart 7).

Electron localization function analysis of the complete wave functions on [$Fe_2(CO)_9$] supports this interpretation.[40] Nevertheless, MO studies are not conclusive in this aspect,[2a,3a,41−43] and an interesting controversy arises about whether the Fe−Fe bond exists. The new compounds **4** and

(36) Bader, R. F. W. *Atoms in Molecules—A Quantum Theory*; Oxford University Press: London, 1990.
(37) Bader, R. F. W.; Johnson, S.; Tang, T. H.; Popelier, P. L. A. *J. Phys. Chem.* **1996**, *100*, 15398.
(38) Bader, R. F. W. *Coord. Chem. Rev.* **2000**, *197*, 71.
(39) Bo, C.; Sarasa, J. P.; Poblet, J. M. *J. Phys. Chem.* **1993**, *97*, 6362.
(40) Kraupp, M. *Chem. Ber.* **1996**, *129*, 527.
(41) Jang, J. H.; Lee, J. G.; Lee, H.; Xie, Y.; Schaeffer, H. F. *J. Phys. Chem. A* **1998**, *102*, 5298.
(42) Salzmann, R.; Kraupp, M.; McMahon, M. T.; Oldfield, E. J. *J. Am. Chem. Soc.* **1998**, *120*, 4771.
(43) Hunstock, E.; Mealli, C.; Calahorda, M. J.; Reinhold, J. *Inorg. Chem.* **1999**, *38*, 5053.

Table 4. Ranges of Values of the Electronic Density (eÅ^{-3}), Laplacian and Ellipticity at the BCPs for Non-bridging Ligands' bonds in Compounds **4a** and **5**

	ρ	$\nabla^2\rho$	ϵ
C−H	0.304 ± 0.003	−1.36 ± 0.02	<0.01
C−F	0.237 ± 0.005	−0.07 ± 0.03	0.24 ± 0.01
C−As	0.141 ± 0.004	−0.08 ± 0.01	<0.03
Fe−As	0.068 ± 0.004	+0.13 ± 0.01	0.05 ± 0.02
Fe−CO (terminal)	0.15 ± 0.02	+0.63 ± 0.03	0.08 ± 0.003
C−O (terminal)[a]	0.47 ± 0.01	+0.46 ± 0.07	≤ 0.03

[a] Because of their special characteristics, terminal carbonyls CO(5) and CO(6) belonging to **5** have been moved to Table 5 and are not considered in the intervals.

Chart 7. Bonding Schemes for Diiron Carbonyl Complexes Arising from the 18-Electron Rule and AIM Calculations

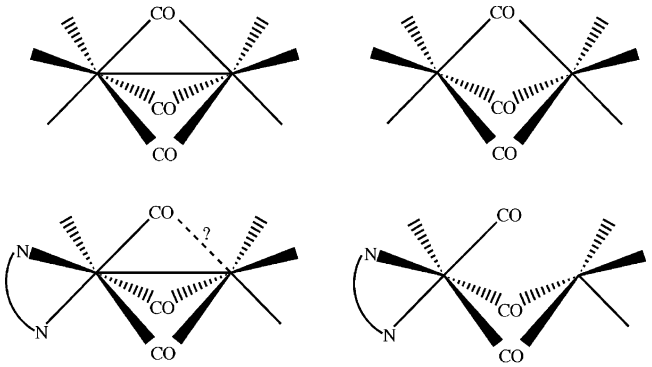

5 offer a good opportunity to investigate the bulk electronic density of diiron carbonyl derivatives with similar external structures but with one different bridging ligand in their core.

The AIM analyses of **4a** and **5** show the common trends found for diiron carbonyl derivatives.[12] The BCP electronic density parameters for the C−H, C−F, and C−As bonds (see Table 4) are closely similar in both compounds and lie inside the normal ranges described in the literature for classical bonds. All of them show negative Laplacian values, which indicate a local electronic density concentration at the BCPs, as expected for bonds with a dominant σ-overlap. The C−H BCPs are that of highest-electronic density values and the most-negative Laplacians, whereas the C−As BCPs have small values, corresponding to strong and weak bonds respectively; their small ellipticities indicate a dominant σ-overlap. Comparatively, the C−F BCPs of the bridging difluoromethylenes show very high ellipticities, being indicative of significant π-bond character: this confirms the good efficiency of these heteroallylic bridges as π-acceptors, as stated in previous works.[15]

With the only exception of the C(6)−O(6) bond in **5**, all of the Fe−As, Fe−C, and CO BCPs in both compounds show positive Laplacian values (see Tables 4 and 5), indicating that they are placed in a local density depletion. This distinctive characteristic was detected in a previous work[12] for bonds involved in a π-back-bonding mechanism: the non-negligible component of the orbital overlap that lies outside of the internuclear line could explain the local depletion of the electronic density on the internuclear line where BCPs are placed.

Table 5. Values of the Electronic Density (e Å^{-3}), Laplacian, and Ellipticity at the BCPs for Bridging Ligand Bonds in Compounds **4a** and **5**

	4a			**5**		
bond[a]	ρ	$\nabla^2\rho$	ϵ	ρ	$\nabla^2\rho$	ϵ
Fe(X)−CF_2	0.113	+0.237	0.035	0.127	+0.238	0.031
CF_2−Fe(Y)	0.109	+0.214	0.043	0.114	+0.237	0.024
Fe(X)−CO(A)	0.123	+0.305	0.070	0.113	+0.288	0.053
CO(A)−Fe(Y)	0.094	+0.205	0.029	0.100	+0.223	0.051
Fe(X)−CO(B)	0.092	+0.205	0.033	0.073	+0.150	0.029
CO(B)−Fe(Y)	0.122	+0.302	0.068	0.141	+0.397	0.102
C−O (A)	0.425	+0.198	0.022	0.428	+0.240	0.029
C−O (B)	0.436	+0.288	0.020	0.419	+0.120	0.018
C(5)−O(5) (terminal)				0.439	+0.206	0.003
C(6)−O(6) (terminal)				0.413	−0.028	0.002

[a] X = 1 for **4a** and 2 for **5**. Y = 2 for **4a** and 1 for **5**. A = 2 for **4a** and 1 for **5**. B = 3 for **4a** and 2 for **5**.

As can be seen in Tables 4 and 5, C−O BCPs in carbonyl ligands show the highest-electronic density values, which are indicative of the strength of the triple bonds. Density and Laplacian values corresponding to the bridging BCPs (see Table 5) are less intense than those of the terminal ones (see Table 4). This bond weakening is attributable to both the loss of internal bond density to establish two σ-donations toward the bridged iron atoms, and the double back-donations from the two metals to the CO antibonding orbitals. For the ellipticity, terminal CO BCPs have values below 0.003, indicating a cylindrical distribution of the electronic density around the bondpath (the addition of one σ- and two perpendicular π-bond densities). For the bridging carbonyls, ellipticity raises 1 order of magnitude, thus indicating a dominant double-bond character caused by the preferential back-donation to the antibonding orbital inside the Fe−CO−Fe plane.

As noted before, terminal CO(6) and CO(5) carbonyls belonging to **5** do not follow the preceding trends: although their BCPs have extremely low ellipticities, the small electronic density, Laplacian values, and crystallographic bond distances are comparable to those of bridging carbonyls, so they have been included with them in Table 5. CO(6) has the most anomalous triple-bond distances, which could be related to its involvement in an intermolecular O(6)···H(73)−C(7) weak hydrogen bond (2.377 Å, 147.4(7)°) with the (x, y, z − 1) neighboring moiety. Because electronic density calculations have been performed on isolated molecules, they cannot properly account for the effect of this intermolecular interaction.

If we focus on the iron atoms coordination environments, the Fe−As BCPs have the weakest-electronic densities, pointing to some lability of the arsine ligands. The Fe−C BCPs have higher densities, similar to those found in related complexes,[12] and they decrease in the order Fe−CO (terminal) > Fe−CF_2 (bridging) ≈ Fe−CO (bridging). The latter comparison confirms the good efficiency of the difluoromethylene fragment as a bridging ligand.[15]

A more detailed inspection of the electronic density inside the dinuclear cores in **4a** and **5** requires the use of a common

Chart 8. Alternative Views for Complexes **4a** and **5** Where Strong and Weak Bridging Bonds Are Equally Oriented, Leading to a Common Labelling Scheme for Table 5

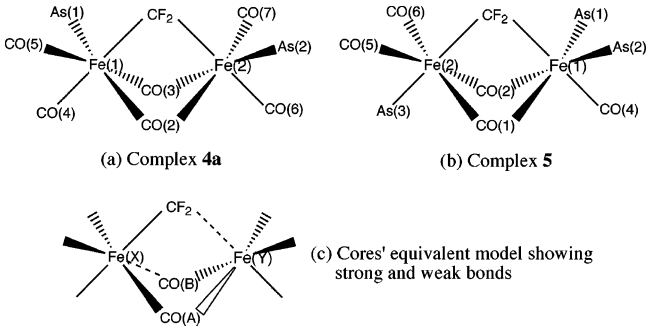

labeling scheme. For both complexes, each bridging ligand is connected to the two iron atoms through nonequal bonds, one shorter than the other. Consequently, molecules must be reoriented in such a way that strong and weak bringing branches coincide to compare them properly: this has been done as indicated in Chart 8. This labeling scheme is used in Table 5.

The core of **4a** contains the most-symmetrical bridging ligand, the CF_2 moiety. This group binds to both irons through two BCPs which densities are less than 5% different. On the contrary, their two bridging carbonyls are clearly asymmetric, as the BCP densities at both sides differ more than 30%. Each iron atom is connected to the two CO bridges through one high-density and one low-density BCP. It is worth noting that the arsine ligands are placed trans to the strong bridging bonds (see Chart 4), so they receive little back-bonding density as deduced from their BCP properties.

The core of **5** is quite similar, although it has a less symmetrical CF_2 bridge (BCP densities differ by 11%) with two different ligands in their trans positions. CO(1) is the less asymmetrical bridging carbonyl, as its two BCP densities differ only by 13%; the densest bondpath is connected to Fe(2) and its trans position is occupied by the anomalous terminal carbonyl CO(6). Conversely, the CO(2) ligand is the most asymmetrical bridging carbonyl: the ratio between its two BCP densities approaches 2:1, thus resulting in a semibridging carbonyl. Fe(2)−CO(2) is the weakest bridging bond, which has the second anomalous terminal carbonyl CO(5) in a trans position (see Chart 6). It can be guessed that Fe(2) spends little electronic density to establish the very weak bridging bond with CO(2), so it can use the surplus to reinforce the bonds with the terminal CO(5) ligand through supplementary back-bonding donation. This would cause the weakening of the internal C−O bonds with conservation of the low ellipticity.

For both cores, six BCPs connecting the iron atoms and the bridging ligands have been found. Their bondpath connectivities clearly define a closed Fe_2C_3 structure and three different Fe_2C_2 four-membered rings. This electronic topology should imply the presence of one cage critical point (CCP) and three ring critical points (RCPs) close to the molecular center. Nevertheless, calculations are unable to find all of them: only two very close ring critical points (0.3 Å apart) are found in that region for **4a** and **5**, with

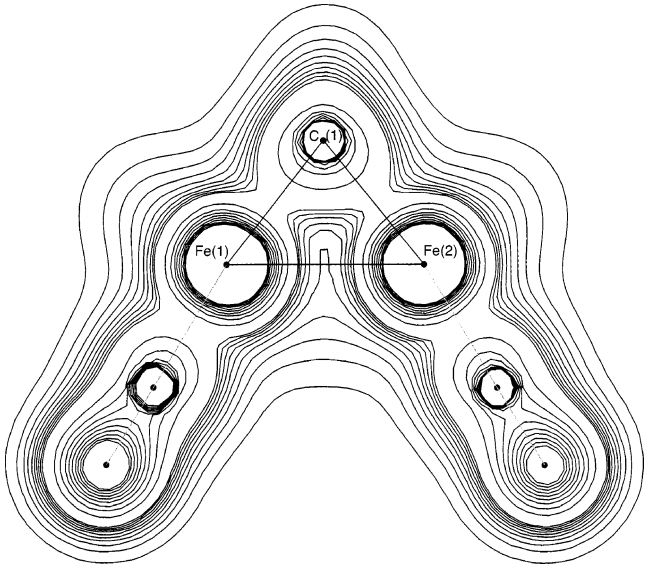

Figure 5. Contour plot for the electronic density of the CF_2 bridge in compound **4a** across the Fe(1)−C(1)−Fe(2) plane. External lines step 0.01 e Å^{-3} and involve the weak bridging bonds. Internal lines step 0.10 e Å^{-3} and correspond to strong bonds and atomic cores. Terminal carbonyls are not in-plane and may appear distorted.

almost identical electronic properties ($\rho = 0.049$ au, $\nabla^2\rho = +0.13$ au), indicating low density and moderate charge depletion. Although the relations between the number of critical points computed for both molecules satisfy the Hopf−Poincaré rule, (n attractors) − (n + 1 BPCs) + 2 RCPs − 0 CCPs = 1 (with $n = 43$ for **4a** and $n = 54$ for **5**), they are not congruent with the bondpath topology, so a third RCP and a CCP must be present in both.

The contour maps of electronic density shown in Figures 5 and 6 for complex **4a** (they are very similar for **5**) illustrate how the core center consists of a region with small and short-ranged density values. The analysis of the Laplacian (see Figure 7) shows continuously positive values across the Fe−Fe line for the outer shell of the metals, reaching a (3, +3) critical point (a minimum of charge depletion with $\nabla^2\rho = +0.121$ au and $\rho = 0.049$ au) close to the core center and inside a region of highly uniform values. Consequently, it is highly probable that both the missed third RCP and CCP would be closely located, together with the two detected RCPs, inside a zone of weak and homogeneous density and Laplacian. As the four expected CPs would be feebly distinguishable, it is reasonable that gradient search methods fail to fix the two missing ones.

In summary, the AIM analysis of the complexes indicates that there is no direct σ-bonding interaction between the two iron atoms inside the dinuclear complexes. This supports the leading rule of the CO and CF_2 bridges in keeping the dinuclear integrity found from MO analysis in similar compounds.[15] Nevertheless, this analysis does not exclude the presence of a direct π-overlap between the two metals, for which no density along the Fe−Fe line is necessary. As its density would be superimposed to that of the bonds with carbonyl and difluoromethylene bridges, its existence would be very difficult to characterize from electronic density analysis.

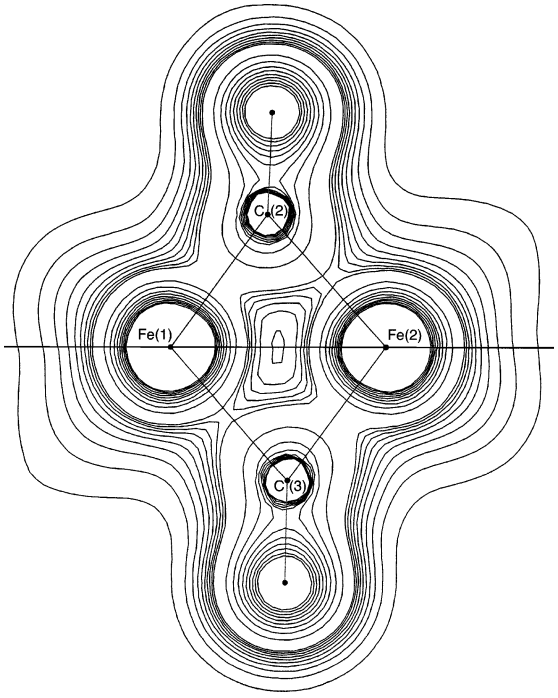

Figure 6. Contour plots for the electronic density of the carbonyl bridges in compound **4a** across the Fe(1)−C(2)−Fe(2) (upper half) and Fe(1)−C(3)−Fe(2) (lower half) planes. External lines step 0.01 e $Å^{-3}$ and involve the weak bridging bonds. Internal lines step 0.10 e $Å^{-3}$ and correspond to strong bonds and atomic cores. Oxygen atoms are not in-plane and may appear distorted.

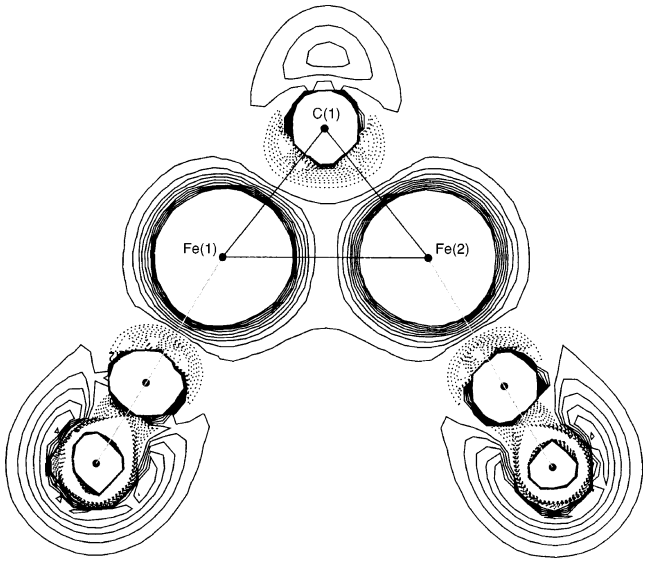

Figure 7. Contour plot of the Laplacian of the electronic density (step 0.01 au) for the internuclear Fe−Fe line in compound **4a** across the Fe(1)−C(1)−Fe(2) plane. Continuous and dashed lines correspond to positive and negative values, respectively. Terminal carbonyls are not in-plane and may appear distorted.

Computational Details. DFT-B3LYP[44−46] single-point calculations were run over the crystallographic geometry (with no optimization) of the compounds **4a** (atoms with occupancy factor 0.25 or less were excluded) and **5** with the Gaussian 98 code[47] on an IBM RS/6000 3AT workstation. The 6-3111+G basis set was applied for the iron centers, whereas for the rest of the atoms, the 6-311G* basis set was used. Wave function files were treated with the AIMPAC[48] suite of programs, modified to account for the input size. Electronic density and Laplacian values were analyzed using the standard built-in parameters. Graphical representations were performed by means of the MOLDEN software.[49]

Conclusion

The replacement of one bridging CO ligand in $[Fe_2(CO)_9]$ by the CF_2 ligand has not only a dramatic influence on the structure but also on the reactivity of the resulting complex **2** toward the usual donor ligands. The mechanism of the reaction of **2** with donor ligands is not yet understood and seems to be very complicated. One reason for the different manner of the reaction may be that $[Fe_2(CO)_9]$ is easily degraded in solution into $[Fe(CO)_4]$ and $[Fe(CO)_5]$ which represent the real reaction partners in substitution processes. Rapid reaction of the 16-electron fragment followed by reaction with $[Fe(CO)_5]$ or a further $[Fe(CO)_4]$ species probably is a key step for the formation of all $[Fe_2(CO)_x(D)_y]$ or $[Fe_2(CO)_x(D-D)_y]$ complexes or even cluster compounds. A related splitting of **2** into $[Fe(CO)_4]$ and $[Fe(CO)_4CF_2]$ is probably less favorable because of the stronger bond of the CF_2 ligand to both iron atoms and the tendency of the latter fragment to dimerize with loss of CO to give $[Fe_2(CO)_7(CF_2)_2]$ (**1**). However, **1** could not be isolated in any of the runs described here. This is a strong argument against such a splitting. One strategy may be in stabilization of a mononuclear CF_2 containing fragment or a $[Fe_2(CO)_x(CF_2)(D)_y]$ species by addition of stronger donor ligands containing more bulky substituents at the donor atoms. The reason that the disubstituted product in the case of $AsMe_3$ forms a type **C-I** species (as in **4**) and in the case of PPh_3 a type **C-II** species (as in **3**) is as yet unclear: one explanation may be that the bulkiness of the phenyl rings may cause the iron atoms to separate more than with the smaller methyl groups of $AsMe_3$. However, electronic reasons cannot be excluded, and further studies are to be done.

Although we have found the shortest Fe−Fe distances of 2.47 Å in **4** and **5**, which are derived from the $[Fe_2(CO)_9]$ structure by replacing bridging and terminal CO groups by other two electron donors, a direct Fe−Fe σ-bond is not

(44) Kohn, W.; Sham, L. J. *Phys. Rev.* **1965**, *140*, A1133.
(45) Becke, A. D. *J. Chem. Phys.* **1993**, *98*, 5648.
(46) Lee, C.; Yang, W.; Parr, R. G. *Phys. Rev. B* **1982**, *37*, 785.
(47) Frisch, M. J.; Trucks, G. W.; Schlegel, H. B.; Scuseria, G. E.; Robb, M. A.; Cheeseman, J. R.; Zakrzewski, V. G.; Montgomery, J. A., Jr.; Stratmann, R. E.; Burant, J. C.; Dapprich, S.; Millam, J. M.; Daniels, A. D.; Kudin, K. N.; Strain, M. C.; Farkas, O.; Tomasi, J.; Barone, V.; Cossi, M.; Cammi, R.; Mennucci, B.; Pomelli, C.; Adamo, C.; Clifford, S.; Ochterski, J.; Petersson, G. A.; Ayala, P. Y.; Cui, Q.; Morokuma, K.; Malick, D. K.; Rabuck, A. D.; Raghavachari, K.; Foresman, J. B.; Cioslowski, J.; Ortiz, J. V.; Stefanov, B. B.; Liu, G.; Liashenko, A.; Piskorz, P.; Komaromi, I.; Gomperts, R.; Martin, R. L.; Fox, D. J.; Keith, T.; Al-Laham, M. A.; Peng, C. Y.; Nanayakkara, A.; Gonzalez, C.; Challacombe, M.; Gill, P. M. W.; Johnson, B. G.; Chen, W.; Wong, M. W.; Andres, J. L.; Head-Gordon, M.; Replogle, E. S.; Pople, J. A. *Gaussian 98*, revision A.7; Gaussian, Inc.: Pittsburgh, PA, 1998.
(48) Biegler-Konig, F. W.; Bader, R. F. W.; Tang, T. *J. Comput. Chem.* **1982**, *3*, 317.
(49) Schaftenaar, G. *MOLDEN, A package for displaying molecular density*; CMB1, University of Nijmegen: Nijmegen, The Netherlands, 1991.

operative as shown by AIM calculations; however, the description of this bond with a π-interaction seems more realistic and is supported by the calculations and the line drawn between the two metals may be interpreted in this sense.

Experimental Section

General Considerations. All operations were carried out under an argon atmosphere in dried and degassed solvents using Schlenk techniques. IR spectra were run on a Nicolet 510 spectrometer. ^{19}F NMR and ^{31}P NMR spectra were recorded on a Bruker AC 300 instrument using $CFCl_3$ and H_3PO_4 (0.00 ppm) as the external standard. Elemental analyses were performed by the analytical service of the Fachbereich Chemie der Universität Marburg (Germany). Although crystalline samples packed under Ar were provided, unsatisfactory results were obtained because of the incomplete combustion despite the wide range of catalyzers assayed. The starting complex **2** has been prepared according to a published procedure.[15] $AsMe_3$ and $AsPr^i_3$ were prepared by known procedures,[50] as were the chelating ligands $Ph_2PCH_2PPh_2$ (dppm) and $Ph_2P(CH_2)_2PPh_2$ (dppe).[51] The ligands bpy and phen were commercially available; anhydrous trimethylaminoxid (TMNO) was obtained from Aldrich as the dihydrate and dehydrated by vacuum sublimation.

Reaction of 2 with bpy. A solution of 2,2′-bpy (266 mg, 0.95 mmol) in THF and a suspension of TMNO (130 mg, 1.70 mmol) were added to a precooled solution of **2** (330 mg, 0.84 mmol) in THF at −25 °C. The mixture was stirred for several hours (until the ^{19}F NMR remained unchanged), during that time a red-brown precipitate formed which then was filtered off and evaporated to dryness. Although several routes to recrystallize the solid were tried using THF, toluene, hexane, and *n*-pentane, no crystals suitable for an X-ray analysis were obtained. IR (Nujol mull): 2060 m, sh 1971 vs, 1930 vs, 1911 vs, 1763 vw, 1089 vw, 1039 w cm^{-1}. The remaining solution showed a ^{19}F NMR signal at 9.70 ppm.

Reaction of 2 with phen. A solution of phen (200 mg, 1.10 mmol) in THF and a suspension of TMNO (173 mg, 2.30 mmol) were added to a precooled solution of **2** (440 mg, 1.15 mmol) in THF at −25 °C. The mixture was stirred for several hours (until the ^{19}F NMR remained unchanged) and then filtered off and evaporated to dryness. As with the bpy reaction product, no crystals were obtained. For the solid, IR (KBr): 2021 s, 1971 vs, 1930 vs, 1905 vs, 1768 vw, 1038 m cm^{-1}. For the solution, ^{19}F NMR: 9.50 ppm. The recrystallization of the solid in CH_2Cl_2 resulted in red crystals of $[Fe(phen)_3]Cl_2$ (**7**) being obtained in about a 2% yield. IR (Nujol mull): 1599 w, 1574 w, 1512 w, 1425 m, 1343 w, 1289 w, 1223 w, 1138 m, 1094 m, 851 s, 804 w, 723 s, 692 w cm^{-1}. During recrystallization of the solid in THF/*n*-pentane, the product finally decomposes, and $[Fe(CO)_3(phen)]$ was obtained and identified by its IR spectrum.[12]

Reaction of 2 with $AsMe_3$. A solution of **2** (345 mg, 0.87 mmol) in ether was layered with a solution of excess $AsMe_3$, and the mixture was allowed to react for several hours until the signal at 49.8 ppm in the ^{19}F NMR of **2** disappeared. Immediately the formation of a precipitate was observed. The product was identified as containing $[Fe_2(\mu\text{-}CF_2)(CO)_6(AsMe_3)_2]$ (**4**) by its IR spectrum. The solution was filtered, concentrated, and layered with *n*-pentane. A mixture of $[Fe_2(\mu\text{-}CF_2)(CO)_6(AsMe_3)_2]$ (**4**) and $[Fe_2(\mu\text{-}CF_2)(CO)_5(AsMe_3)_3]$ (**5**) was obtained, and the crystals were separated mechanically. Yield for **4**: 80 mg (0.14 mmol, 16%). Analyses: H, 2.89 (3.18); C, 26.11 (27.40)%. Yield for **5**: 55 mg (0.08 mmol, 9%). Analyses: H, 4.30 (4.11); C, 26.38 (27.20)%. The IR spectra (Nujol mull) of **4** and **5** are collected in Table 1. Further efforts to manipulate the precipitate resulted in insoluble decomposition products being obtained. The solubility of **4** and **5** is low in common solvents.

Reaction of 2 with $AsPr^i_3$. A solution of **2** (320 mg, 0.83 mmol) in ether was layered with a solution of excess $AsPr^i_3$ and allowed to react for several hours until the signal at 49.8 ppm in the ^{19}F NMR of **2** disappeared and one signal at 42 ppm appeared. The majority of the obtained product precipitates in the reaction mixture. Further efforts to manipulate the solid resulted in insoluble decomposition products being obtained. IR (Nujol mull) of the precipitate: 2042 m, 2010 w, 1986 w, 1966 m, 1931 vs, 1862 s cm^{-1}.

Reaction of 2 with $Ph_2PCH_2PPh_2$ (dppm). An equimolar mixture of **2** (320 mg, 0.84 mmol) and dppm (440 mg, 0.84 mmol) in toluene was stirred for several hours at 50 °C. The mixture was filtered off and evaporated to dryness. The residue was redissolved with toluene and layered with *n*-pentane. After several recrystallizations from THF/*n*-pentane, some red crystals of $[Fe_2(\mu\text{-dppm})_2(CO)_5]\cdot MeC_6H_5$ (**6**$\cdot MeC_6H_5$) were isolated (yield below 5%). IR (Nujol mull): 2025 w, 1987 w, 1923 m, 1901 s, 1873 s, 1854 s, 1682 s, 1603 w, 1588 w, 1574 w, 1495 w, 1485 m, 1435 s, 1366 m, 1333 w, 1310 w, 1277 w, 1190 w, 1161 w, 1127 w, 1094 s, 1082 w, 1001 w, 789 s, 764 m, 735 s, 692 s, 625 s, 592 m, 565 m, 515 s, 490 s cm^{-1}. Analyses: H, 4.48 (4.71); C, 65.90 (66.92)%.

Reaction of 2 with $Ph_2PCH_2CH_2PPh_2$ (dppe). A solution of dppe (460 mg, 0.85 mmol) in toluene and TMNO (1.70 mmol) were added to a solution of **2** (330 mg, 0.85 mmol) in toluene. The mixture was stirred at room temperature and allowed to react for several hours until the ^{19}F and ^{31}P NMR remained unchanged. The solution was filtered off and evaporated to dryness. Effort to recrystallize the residue gave decomposition products. ^{19}F NMR (toluene): δ 35. ^{31}P NMR: δ 96. IR (Nujol mull): 2046 m, 2005 s, 1975 vs, 1887 m, 1831 w, 1789 w, 1018 m, 952 m cm^{-1}.

Acknowledgment. We thank the Deutsche Forschungsgemeinschaft for financial support. We are also grateful to the Fonds der Chemischen Industrie, Frankfurt/Main, Germany, and the Max-Planck-Society, Munich, Germany, for financial support. M.D.V. was partially funded by scholarship from the Universitat de Barcelona. M.D.V. and R.C. thank the Ministerio de Education y Ciencia for financial support (Grants BQU2003/00539 and CTQ2005-08459-C02-01, respectively).

Supporting Information Available: Tables of atomic positions, equivalent isotropic thermal parameters, and anisotropic thermal displacement coefficients. This material is available free of charge via the Internet at http://pubs.acs.org. The crystallographic data have been deposited as supplementary publications CCDC-292781 (**4**), -292780 (**5**), -292782 (**6**), and -292783 (**7**) at the Cambridge Crystallographic Data Center. Copies of the data can be ordered from CCDC, 12 Union Road, Cambridge CB2 1EZ, U.K. (e-mail: deposit@ccdc.cam.ac.uk).

IC0604011

(50) Claeys, E. G. *J. Organomet. Chem.* **1966**, *5*, 446.
(51) Issleib, K.; Müller, D.-W. *Chem. Ber*. **1959**, *92*, 3175.
(52) Sheldrick, G. M. *SHELXL-97*; Universität Göttingen: Göttingen, Germany, 1997.
(53) Sheldrick, G. M. *SHELXS-97*; Universität Göttingen: Göttingen, Germany, 1997.